Chapter 7

RSSI/DoA Based Positioning Systems for Wireless Sensor Network

Stefano Maddio, Alessandro Cidronali and Gianfranco Manes

Additional information is available at the end of the chapter

http://dx.doi.org/10.5772/50380

1. Introduction

The problem of localization of a mobile device has interested researchers since the beginning of XX century, as testified by the experiments of Bellini and Tosi [20]. This challenging research topic has gained even more momentum in recent years, particularly with the introduction of modern ICT technologies such as Wireless Sensor Network (WSN).

A Wireless Sensor Network is an infrastructure comprised of a set independent nodes able to sense (measure), process and communicate among themselves and toward a remote sink node which operates as data aggregator and forwards the information to the final user. WSN are already actively employed in unattended and non-invasive activities like prevention of art deterioration [1, 23], agricultural monitoring [18], environment monitoring [17, 22], surveillance application [2, 10]. In most cases, if not in all cases, it is necessary to report the measured data to the position of the observed phenomenon, otherwise the measurement would be meaningless. This means that the sensor nodes have to be aware of their position, and if this information is not known, a *localization service* must be implemented. The *position awareness* that comes from this service can boost specific routing operations (adaptability, latency, throughput) with the nodes able to independently determine the best modality to cooperate and communicate the data to the end user by means of a continuous exchange of messages.

The objective of a localization system is to assign a positional information to each node of the network, either in the form of a relative position to a known anchor reference of within a coordinate system [7]. A localization procedure can be described as the series of three steps:

- Signal observation
- Extract of position-related signal parameters
- Estimation of location coordinates

A localization strategy is *effective* if accurate for the specific sensing application, and it is *efficient* if operates with minimal (hardware, software, bandwidth) resources. The most popular example of localization system is given by the widespread Global Positioning System (GPS) [7, 12], which allows a mobile node to accurately compute its position using the distances from three or more satellites. Unfortunately, GPS is not always a feasible solution, for cost or power constraints. There are also applications, like communication in indoor area, where GPS fails for physical reasons.

The fundamental principles of localization in a GPS-denied condition have been thoroughly investigated in the literature, but a successful implementation of localization procedure is still challenged by many practical issues. Various strategies has been proposed, relying on several class of data sensors (sound and ultra-sonic, light/laser, inductive/proximity, etc). Among these, the systems capable of performing the positioning service without additional hardware – excluding the communication infrastructure – are particular efficient. COTS devices are already equipped with a *Received Signal Strength Indicator* (RSSI). This kind of device gives access to a power sensor at zero cost, typically in the form of a digital data available on a register. The RSSI collection represent the signal observation phase of the localization procedure.

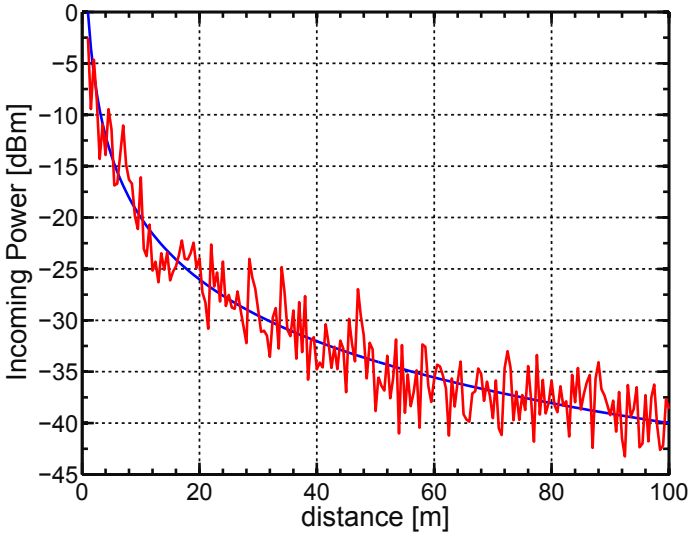

Figure 1. Distance Estimation with Power Measurement. The blue curve has a (theoretical) hyperbolic behavior. The red curve represents the actual behavior.

In the context of the Wireless Sensor Networks, RSSI measurements are already widely used to estimate the *range* – the relative distance – of the sensor nodes. The range estimation, which corresponds to the position-related signal extraction, is based on the fact that the power carried by an RF signal is inversely proportional to the traveled distance. This relationship is graphically described by the blue curve in Figure 1.

When at least three range measurements respect to three reference – non collinear – nodes are available, the estimation of location coordinates is obtained on the basis of trilateration algorithms, graphically described in Figure 2(a). The intersection of three circles, eventually in the mean square error sense, corresponds to the solution of a non-linear system, a trivial numeric elaboration.

Unfortunately, traveling radio signals are influenced by the indoor environment, being strongly affected by the reflected, refracted and scattered waves (multi-path) and disturbed by other devices communications (interferences). The actual power/distance relationship is more similar to the red noisy curve of Figure 1. Because of this noisy behavior, the power estimation is affected by a low accuracy, ultimately leading to a coarse position estimation, as depicted in Figure 2(b). This bad condition can be mitigated if more than three ranges are available, which leads to an overdetermined system (multilateration).

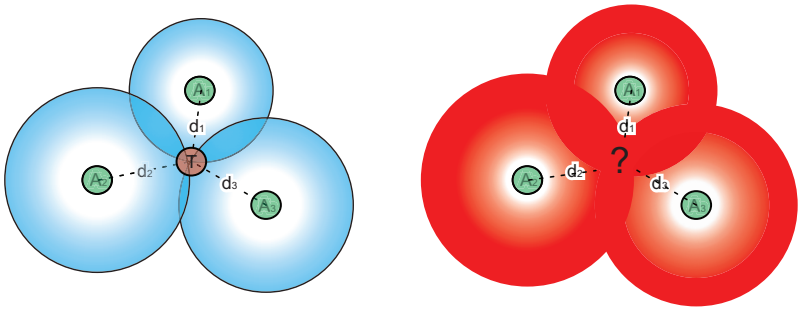

(a) Ideal case (b) Real case

Figure 2. Target localization by trilateration algorithm. The position of a node is determined with three range estimations respect to three reference nodes.

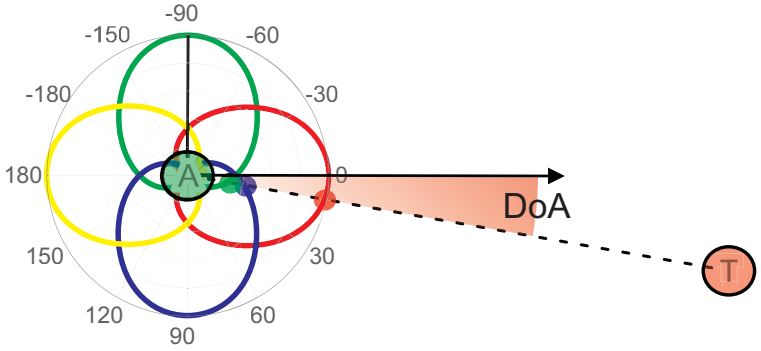

Figure 3. Direction of Arrival estimation with a multi-beam antenna system.

RSSI measurements can also be employed for *Direction of Arrival* (DoA) estimation. A positioning system based on DoA information does not rely on actual range measurements, i.e. it is *range-free* algorithm. The extraction of the signal DoA parameter is based on the

antenna reception with a *multi beam system*, an antenna capable to radiate N directional beam patterns arranged in a sectorialised manner. The logic is to sense a power vector from different direction, as explained by Figure 3. Intuitively, if each beam is narrow enough, the antenna operates as a *spatial filter*, isolating a specific angular region. This estimation procedure is tolerant to noisy power measurements, because it has a range-free nature, thus it is particularly suitable for the a coarse power meter like RSSI. The critical condition for is the need of a *fast scanning* of the available beam, to ensure the same channel condition through the N antenna beams. For a DoA based algorithm, the estimation of position coordinates relies on the collaboration of at least two nodes operating as *beacons*, as explained in Figure 4. Each anchor estimates the DoA of the target respect to its relative reference, identifying a *line of bearing*. The intersection of two lines uniquely identify the target position. As for the multilateration, the collaboration of three or more anchors can enhance the estimation effectiveness.

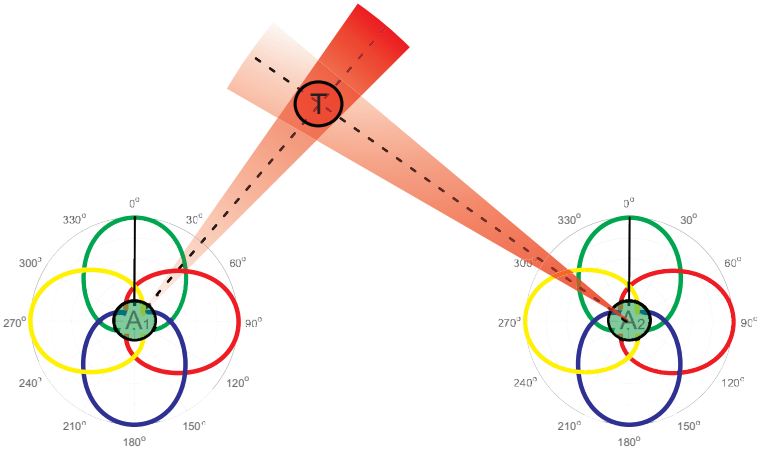

Figure 4. Target localization by DoA intersection. The estimated position does not rely on range measurement.

2. Node design

This section describes a brief summary of the typical hardware of a a sensor node suitable for the described RSSI/DoA-based localization system. The idea is to use two class of nodes. The master node, designed with a system consisting of a transceiver and a micro-controller as the core intelligence and equipped with the complex radiative system. The slave node, based on analogous but simplified design and equipped with a simple antenna. The master (anchor) node can be thought as the sink/coordinator, a specialized node, eventually placed by hand, serving as an access point. The slave (target) node, is the independent node, eventually free to move in the area within the communication range of at least one master node.

Recent advances in RFIC design opened the door to low-cost commercial transceiver technology. The CC2430 from Texas Instruments is a true System-on-Chip (SoC), an highly integrated RF chip built in 0.18 μm CMOS standard technology, with a compact 7×7 mm QLP48 package. CC2430 comes with an excellent transceiver, boosted with 2.4GHz DSSS

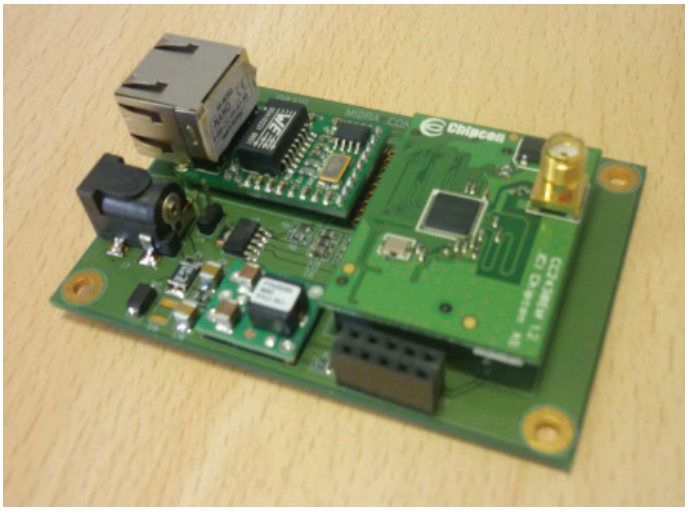

Figure 5. Node main board. The CC2430, the Ethernet module, the power plug and the I/O pins are visible.

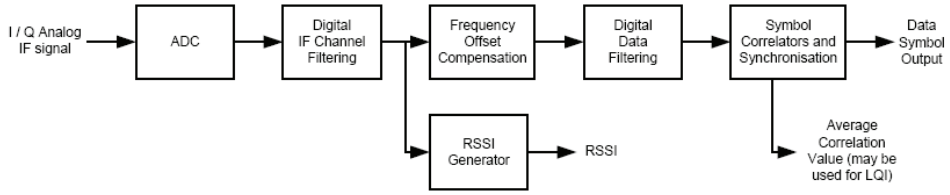

Figure 6. Internal structure of CC2430 demodulator, taken from CC2430 datasheet.

(Direct Sequence Spread Spectrum) operation which is IEEE 802.15.4 compliant, with an high sensitivity, suitable for operation with the ZigBee protocol. The embedded 8-bit core is compatible with the high performance and efficient 8051 industrial controller, with an embedded in-system programmable flash memory of 32, 64 or 128 Kbyte, 8 KB RAM and many other sensors and peripherals, such as analog-digital converter (ADC), several timers, AES128 coprocessor, watchdog timer, 32 kHz crystal oscillator with sleep mode timer, and 21 digital pins, which can be accessed by peripherals to manage I/O operations.

This SoC is also suitable for low-power operation, with a current consumption below 27 mA in either transmitting or receiving mode, while providing a wide supply voltage range (2.0 V - 3.6 V). A battery monitoring with temperature sensing is also integrated. Very fast transition times from low-power modes (0.3 μA in stand-by mode and 0.5 μA in powerdown mode) to active mode enables ultra low average power consumption in low duty-cycle systems, making CC2430 especially suitable for the applications which requires the battery's life is very long. Thanks to this impressive hardware architecture and the compatibility with the Zigbee protocol, this SoC is already a perfect candidate to build any kind of WSN node with only a few Components-Off-The-Shelf (COTS) external hardware. A detail of the CC2430's internal structure is shown as Figure6.

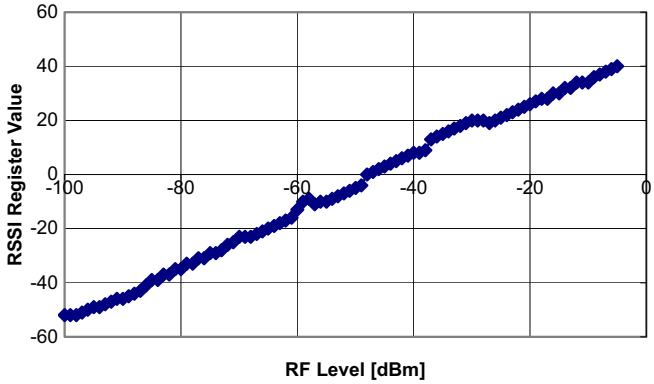

Figure 7. Typical RSSI behaviour, taken from CC2430 datasheet. RSSI_{REG} vs actual received power on the RF pin.

2.1. Received Signal Strength Indicator

Among the other interesting features of this module there is the independent setting of the output power in accord with the external needs (through the action of the micro), and the built-in RSSI (Received Signal Strength Indicator) and LQI (Link Quality Indicator) indexes, always available to the micro, and so to the user via I/O ports. The built-in RSSI module operate averaging the received signal energy over an 8 symbol periods (128 μs) and return this value in the form of a formatted data register, in accord with the IEEE protocol. This 8-bit data is related to the effective incoming power through an equation provided by the manufacturer. The actual impinging power at the RF pin is expressed by (in dBm):

$$P_{in} = RSSI_{REG} + RSSI_{OFFSET} \tag{1}$$

that is, a linear combination of a constant bias value, and the sensed RSSI available on the register. Unfortunately this simple expression is a fitting where the $RSSI_{OFFSET}$ is found empirically around -45 dBm, but experiments reveals a variance of 2 or 3 dB. Even the linear behavior is a fitting, since experiment shows deviation even in cabled link. Nevertheless, the adoption of a built-in RSSI module permits hardware simplification and development time reduction, relaxing the hardware costs.

3. Switched beam antennas

The use of *smart antennas* improves the performance of wireless sensor network in several ways. Smart antennas technology has been introduced in the world of wireless communication system for two main reasons: alleviate the problems of limited performance of omni-directional radiators and gain the ability to perform operation otherwise impossible for canonical antenna.

The problem of limited resource in term of available power can be brilliantly solved with the aid of a spatial diversity system, an antenna system able to radiate power only where is needed, avoiding waste of power. Directional antenna allows a better efficiency for the power utilization, since the same received power is obtained with less transmission power,

or, alternatively, greater transmission range with the same available power. The ability to reach longer range, focusing the available power only in the specific direction of the listener, is another great benefit paired with the reduced energy consumption. Another benefit of the spatial filtering nature of directive links, is the reduction of co-channel interference, since two transmitter in the same area can perform a communication task in two different directions on the same frequency band avoiding influence. This feature can solve the problem of clash and consequently idle time even in a dense transmission area. Another consequence of the latter is the spatial re-usability which can be exploited to increase network capacity and throughput [17].

In the general case, when the relative positions of transmitter and receiver are not known, a single directive antenna responsible for only a specific directional beam, is not enough. To cover the entire angular domain without losing the advantages of directive beams, a more complex structure is required, made of more elementary antennas appropriately arranged. The disadvantage is that this structure could become cumbersome if the size of the antenna is large. However, operating at a center frequency of 2.45 GHz, the need to compensate for the severe path loss multiple directional antenna makes the system a reasonable compromise. In addition, the radiative structure can be possibly be used shelter of the node itself. The intrinsically efficient power management have made directive antenna already suitable for cellular towers and base stations, where the benefits justify the costs (mobile phone tracking), but the use in WSNs is not equally widespread, mainly because of the need to design specific directional protocols. Nevertheless, directive antennas permits low-cost localization with no additional hardware, moving the balance of costs and benefits.

A *Switched beam antennas* consists of an antenna array fed by a beamforming network and it is capable of a predetermined set of beams which can be selected with an appropriate digital control [6]. This technology is complementary of the *adaptive beamformer*, which is an antenna array combined with a phase-shifting device, able to adaptively generate the required radiation pattern pointing in arbitrary direction. Nevertheless the SBA enables a low-cost, low-complexity solution for WSN based localization system. To ensure adequate reliability and accurate DoA estimation a SBA must fulfill two conditions:

- Each antenna element has to be in its maximum receiving condition when the other are in a null zone in order to have angularly uncorrelated signals at the input of the various elements,
- The opportune domain coverage has to be guaranteed in a cumulative sense.

Typically, the *cumulative* of the SBA radiation patterns has to be almost isotropic, for reason which will be clarified in the following sections.

3.1. Elementary antenna

The suitable elementary radiator of a SBA is *the printed antenna*, a planar radiator realized in the same technology of Printed Circuit Board, and based on the same inexpensive supports. Printed antennas have several attractive properties: they are lightweight, low-profile, compact, cheap, easy to fabricate and that they can be made conformal to the host surface. Patches can assume any arbitrary shapes, making them versatile in terms of resonant frequency, polarization and pattern shaping. Printed antennas operating in their fundamental

resonant mode exhibit a directive pattern, behaving as a broadside radiator, with a gain ranging from 3 to 5 dB, and an half beam angle θ_{HP} ranging from 60 to 90 degrees. Other pattern configuration in term of directivity and θ_{HB} are possible by exploiting the higher resonant modes with the opportune feeding mechanism, or combining more than one in a (sub)array.

It is possible to demonstrate that the variance of the DoA estimation is proportional to RSSI variance [24], hence reducing σ_{RSSI} will directly reduce $\sigma_{\hat{\theta}}$, and therefore the DoA uncertainty. The radio channel dispersion, responsible of the measurement variance, is caused by time-varying multi-path propagation, which can be reduced by a proper choice of *antenna polarization*. It has been demonstrated that antennas operating in *Circular polarization* (CP) are effective in reducing this kind of variance and have been already exploited in wireless system operating indoors, and in radio-positioning applications.

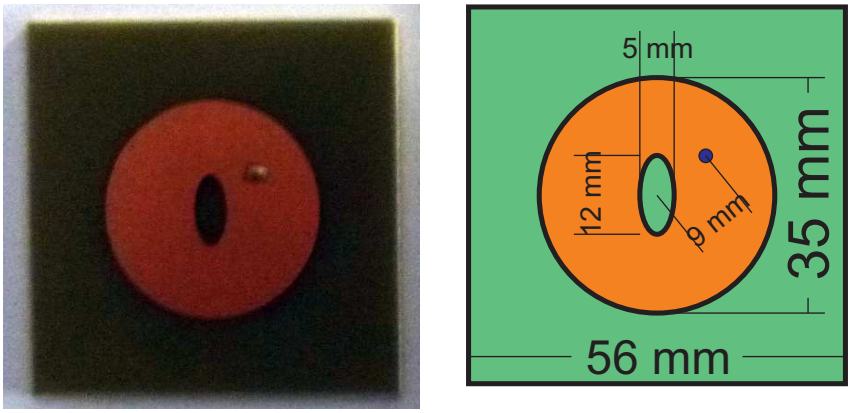

(a) element photograph (b) element design with quotes

Figure 8. An elementary patch radiator suitable for the Switched Beam Antenna.

A smart strategy to design compact CP antennas without an external splitting device is the modal degeneration. A *quasi-symmetrical* shaped patch antenna potentially support circular radiation with a single feed [4, 8]. The proposes radiative system is based on the *Elliptical Slitted Disk Antenna* (ESDA) a disc-based patch antenna working in the fundamental TM_{11} mode and exhibiting a boresight directional radiation pattern [16]. The elliptical slit at the center of the patch serves as the modal degeneration segment. Because of this perturbation, the antenna can sustain two orthogonal detuned modes which exhibit almost the same linearly polarized radiative behavior of a canonic disc working in the fundamental mode. CP radiation is achieved when these two modes, which are orthogonal, combine in phase quadrature with the same magnitude. This type of antenna has been already successfully employed in localization application [5, 6].

The antenna elements are printed over a common cheap FR4 substrate ($\epsilon_r = 4.4$, $h = 1.6\,mm$, 17 μm metalization thickness) shaped in a square geometry. Figure 8(a) shows a photograph of the antenna prototypes. Figure 9 shows the antenna reflection coefficient versus frequency. The 10 dB return loss bandwidth cover the entire ISM band. The antenna pattern is depicted in

cartesian form in Figure 10. The Total gain, Left-Hand gain and Right-Hand gain component are shown. A peak gain of 3.75 dB is achieved in the boresight direction, while the principal lobe shows a θ_{HP} of almost 80 degrees. Co/Cross discrimination is around 20 dB at the gain peak condition.

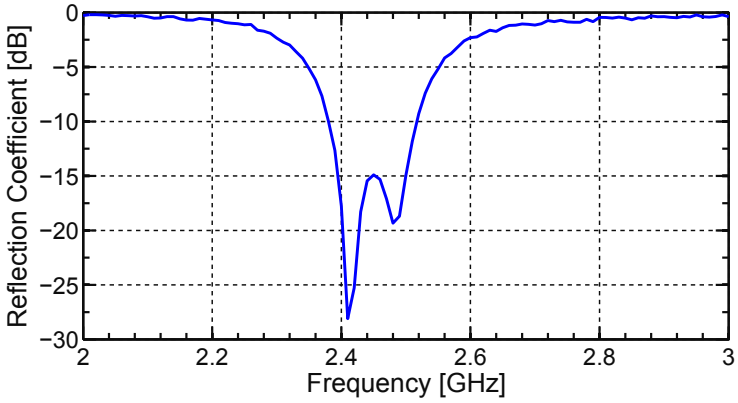

Figure 9. Antenna reflection coefficient versus frequency.

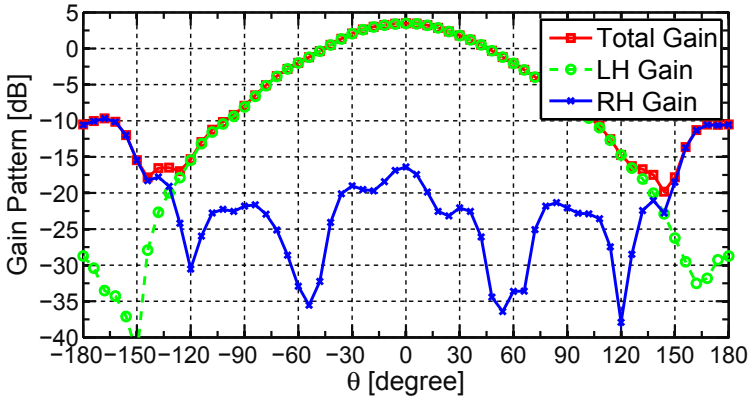

Figure 10. Total, LeftHand and RightHand Antenna Pattern versus Frequency.

3.2. Selection mechanism

The simpler form of RF selection logic is the Single Pole N through (SPNT) switch, directly feeding the N directional antenna (the through) with the the CC RF pin (the pole). The SPNT operation is controlled by the available digital lines taken from the programmable pins of the CC. The RSSI data collection is performed dynamically activating each antenna beam on a scheduling basis, at protocol level.

The adoption of a non-reflective switch is adequate for the SBA operation; the inactive faces are nominally terminated on matched dummy loads without significantly perturbing the

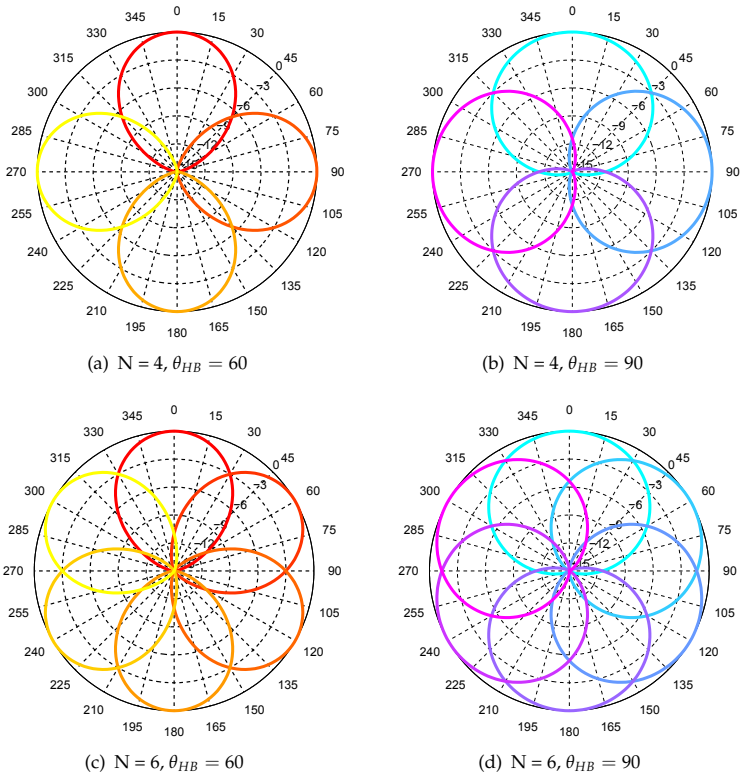

(a) N = 4, $\theta_{HB} = 60$ (b) N = 4, $\theta_{HB} = 90$

(c) N = 6, $\theta_{HB} = 60$ (d) N = 6, $\theta_{HB} = 90$

Figure 11. Regular arrangement of 4 and 6 antenna beams. Each pattern is modeled after Eq. 8, with $\theta_n = {}^{2\pi n}/_{N}$.

radiation pattern of the active element. The drawback of this selection mechanism is the RF loss, which is proportional on N, i.e. on the antenna number. This fact poses a limit to the sensibility of the node. Another problem, is the low isolation of the channels, which could lead to coupling between the antennas, thus affecting the pattern generation, and corrupting the antenna polarization.

A suitable commercial SPNT family is provided by hittite [11]. The HMC family is composed by *non-reflective* SPNT which exhibits moderate insertion loss and adequate isolation for the application in exam. For example the HMC252QS24 SP4T, exhibits moderate insertion loss of 1 dB (over the channels) and an isolation in excess of than 35 dB, is adequate for the application of interest.

4. Localization algorithm

This section describes the algorithmic approach suitable for the proposed localization system. The performances of the localization are based on the SBA characteristics and on the radio channel conditions.

The simplest radio link model is the Friis transmission formula, which relate the received power to the transmitted power as a function of the distance between the source and the destination, as well as of many other link parameters [3, 19]:

$$P_{Rx} = P_{Tx} \frac{G_{Rx}(\bar{\theta}) G_{Tx}(\bar{\theta})}{d^2} \left(\frac{\lambda}{4\pi} \right)^2 \tag{2}$$

where P_{Tx} and P_{Rx} are the transmitted and receiver power, G_{Tx} and G_{Rx} are the transmitter and receiver antenna gains – evaluated in $\bar{\theta}$, the direction of the link – and d is the distance between the units. This expression is valid under the *matching condition* hypothesis, i.e. when each antenna is matched to the respective transceiver and they are also matched in polarization sense. The distance term is referred to the wavelength of the signal, which for the ISM central frequency is equal to:

$$\lambda_0 = \frac{c}{f_0} = \frac{c}{2.45\,GHz} = 0.12\,[m] \tag{3}$$

The free space model is approximatively valid only for communication in the far-field condition, when the distance $d/\lambda_0 >> 1$. The Friis formula is most commonly re-casted in dB form, and in this form it is straightforward to add the mismatches as subtraction terms:

$$P_{Rx} = P_{Tx} + G_{Rx}(\theta) + G_{Tx}(\theta) - R_{LOSS} - T_{LOSS} - X_{LOSS} - PATH_{LOSS} \tag{4}$$

Where T_{LOSS} and R_{LOSS} are the reflection loss of transmitting and receiving antennas, and X_{LOSS} is the antenna polarization mismatch, and each quantity is intended in dB sense. The use of CP antenna is and aid to avoid polarization mismatch since CP antenna communicate independently form their relative orientation. The various loss terms are constant for a fixed pair of transceivers, while the $PATH_{LOSS}$ term is:

$$PATH_{LOSS} = n_p \log(4\pi d/\lambda_0) \tag{5}$$

where n_p, called *loss exponent*, is equal to two only for an unobstructed free space condition. In a more realistic scenario – for example in a complex indoor area – the RF link model cannot be taken as simple as the one expressed by eq. 2. It is still possible consider the model valid, but in a statistical sense, and to better account the higher loss rate, the n_p exponent is raised to three, four or even more. DoA estimation is a range-free algorithm, so it can be implemented with minimal assumptions on the propagation model that relate the RSSI to the distance.

The angular diversity mechanism is exploited by a progressive sensing of the incoming message over the set of available antenna beams. Consider the link of an anchor A and a target T. Upon a request message sent by the anchor, the node T responds with a opportunely repeated broadcast message. The anchor, which is now in monitoring phase, sense the incoming power through the set of its N prefixed beams. Operating on these measurements, node A is able to estimate the DoA of the T respect to its A-centric reference system.

Given the small antenna dimensions, all the faces are at about the same distance from the target: this is the common simplification made in the array theory. According to eq. 4, the received power P_n correspondent to the n^{th} beam is:

$$P_n = P_0 + G_n(\theta) \tag{6}$$

where P_0 is the power of the target's message impinging on the SBA – comprehensive of all the loss terms – while $G_n(\theta)$ is the gain of the n^{th} beam evaluated in the transmission angle, specified to a reference fixed to the anchor node.

Considering Figure 10, an analytical model suitable for the description of the antenna beam is the regular cardioid. A cardioid pattern is identified by its maximum gain, the half-power radiation angle, and the nominal pointing direction specified by θ_0:

$$G(\theta) = G_{max}\left(\frac{1}{2}\left(1+\cos(\theta-\theta_0)\right)\right)^m \tag{7}$$

Where the exponent m is inversely related to the aperture of the beam. This model, while simple, is not unrealistic and it is suitable for numerical implementation [14]. Supposing a regular known arrangement, the nominal pointing direction θ_{n0} of each SBA element is known, and so that the gain pattern of the set of N elements, expressed in dB form:

$$G_n(\theta) = G_{max} + 10m_n \log\left(0.5 + 0.5\cos\left(\theta - \theta_{n0}\right)\right) \tag{8}$$

The radiation pattern of the T node is supposed to be omni-directional, thus it adds the same contribute for each reaching antenna.

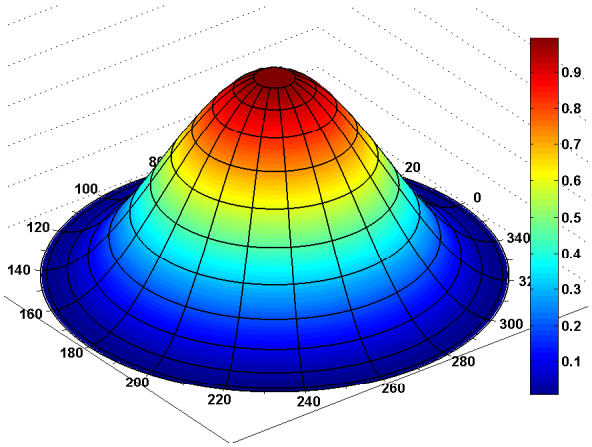

Figure 12. 3D plot of the analytical cardioid model expressed by Eq. 7.

The available data for the algorithm is ultimately a vector of RSSI samples, which can be considered a *function* of the incoming data, as expressed in 2.1:

$$RSSI_n = f\left(G_n(\theta) + P_0 + W_n\right) \qquad n = \{1,\ldots,N\} \tag{9}$$

where W_n is the unavoidable noise term. In a realistic scenario, the noise term accounts also for the RSSI BIAS, with a constant but unknown term, characteristic of the specific device – i.e. $< W_n >= \text{RSSI}_{BIAS}$, $< W_n^2 >= \sigma_W^2$. Typically, the RSSI register is given as an integer. A simple but not unrealistic model for the RSSI is:

$$RSSI_n = \lfloor G_n(\theta) + P_0 + W_n \rfloor \qquad n = \{1,\ldots,N\} \tag{10}$$

where $\lfloor \cdot \rfloor$ is the floor function. Finaly, the RSSI vector are collected in sampled form, with a discretization step ΔT:

$$RSSI_n[k] = RSSI_n(T_0 + k\Delta T) \tag{11}$$

The following section deals with some possible algorithms for the Direction of Arrival estimation, formally identified with $\hat{\theta}$, on the basis of M repetitions of the RSSI vectors. The SBA patterns are supposed to be known and the eventually difference between the nominal and the actual pattern can be considered part of the measurement noise – the *Degree of Imperfection* (DOI).

4.1. Strongest beam

The simplest localization algorithm is based on the classification of the RSSI vector elements. [6, 13]. The Direction of Arrival – which in this case can be more properly defined as the Sector of Arrival – is identified with the antenna domain of the strongest beam, where the n-th antenna domain is defined as the angular range where the n-th antenna gain is higher than the other antennas:

$$\mathcal{D}_i = \{G_j(\theta) > G_i(\theta), \quad j \neq i\} \tag{12}$$

The formal angular estimate is obtained using the reference direction of the antenna that receives the maximum RSSI level, averaged over k = 1...M measures. This estimator comes at zero computational cost, since it consists only in a search and sort of the RSSI vector, and it can be handy as preprocessing stage.

4.2. Least square error

Another estimation strategy is based on the difference between the expected and the actual value [9]. Considering Eq. 10, an *error function* can be defined:

$$\text{err}(\theta) = ||\text{RSSI} - G(\theta)||. \tag{13}$$

This cost function has the form of the N-dimensional error norm, which clearly has a minimum in $\theta = \bar{\theta}$, and this minimum would be nominally equal to the a vector equal to P_0, in the ideal noiseless case. The formal DoA $\hat{\theta}$ can be found by minimizing this cost function in the sense of least square error:

$$\hat{\theta} = \underset{\theta}{\text{argmin}} \left(||\text{RSSI} - G(\theta)|| \right) \tag{14}$$

As a side not, the actual minimum of $||\text{RSSI} - G(\theta)||$ is a vector composed of N repetitions of P_0, therefore it can be used to obtain a range estimation, with a reduced uncertainty with respect to the case of the canonical range estimation approach.

4.3. MUSIC

One of the best algorithm for the DoA estimation with a SBA is based on the *Multiple Signal Classification* (MUSIC) algorithm [13, 21], an array signal processing based on the spectral decomposition of the covariance matrix of the power readings on each face, exploiting the signal space projection properties. Classical MUSIC algorithm for DoA assumed a complex

signal – i.e. module and phase – but a variant where no phase information is required is possible, which means an algorithm based on RSSI only [14, 15, 24].

The MUSIC assumes readings expressed by the following linear model:

$$\begin{bmatrix} y_1[k] \\ \vdots \\ y_N[k] \end{bmatrix} = \begin{bmatrix} G_1(\theta) \\ \vdots \\ G_N(\theta) \end{bmatrix} x[k] + \begin{bmatrix} w_1[k] \\ \vdots \\ w_N[k] \end{bmatrix} \tag{15}$$

where $y_n(m)$ is the power in linear form estimated on face n upon reception of the m^{th} message – $y_n = 10^{(RSSI_n/10)}$ –, while $x(m)$ is the impinging signal affected by a N-dimensional $W(k)$ noise vector.

The data correlation matrix – R_{yy}– estimated on based of K repetitions, is given by:

$$\hat{R}_{yy} = E\left[y[k]y[k]^\top\right] = \frac{1}{K}\sum_{k=1}^{K} y[k]y[k]^\top \tag{16}$$

It is possible to demonstrate that:

$$\hat{R}_{yy} = \sum_{m=i}^{M} \sigma_x^2 G(\theta) + \sigma_w^2 I \tag{17}$$

where $\sigma_x^2 = E|x_n^2[k]|$ is the power of the n^{th} signal and $\sigma_w^2 = E|w_w^2[m]|$ is the noise power. Thus, applying the *single value decomposition*, the set of the following matrices is obtained:

$$R_{yy} = USU^* \tag{18}$$

Considering only an incoming signal, a partition of the space spanned by the columns of $U = [U_x, U_w]$ is obtained: We refer to U_x as the *signal subspace*. Similarly, U_n is the *noise subspace*. Since U is a unitary matrix the signal and noise subspaces are orthogonal, so that $U_x U_n = 0$. Thus we define a *pseudo-spectrum*:

$$\mathrm{P}_{\mathrm{MUSIC}}(\theta) = \frac{1}{G(\theta)U_n} \tag{19}$$

that exhibits a sharp maximum for angle supposedly close to the true DoA, formally identified with:

$$\hat{\theta} = \underset{\theta}{\operatorname{argmax}}\, \mathrm{P}_{\mathrm{MUSIC}}(\theta)\,. \tag{20}$$

5. Simulated experiment

In this section, a set of simulated localization experiments is presented. Each communication process involved in the simulation is modeled after eq. 10, considering also the case of the incoming power lower than receiver sensitivity. The geometrical quantities are analytically determined, and the communication noise is generated as a random number with a Gaussian statistic. Each simulation is parametrized by a set of geometrical, physical and statistical parameters. For the sake of simplicity, the only algorithm considered in the following sections is MUSIC, since it has the best performance/cost trade-off.

If the incoming power is lower than receiver sensitivity, which is around -94 dBm for the system in exam, the only possible conclusion is that the transmitter node is out of the receiver range.

5.1. Single node

To validate our choice, the position of single node located in a unobstructed square area of 10×10 m is considered. At the the corners of the area, four anchors are placed at the distance of 1 m to the boundary wall. Each anchor is equipped with a N-SBA ($N > 2$). Each elementary anchor node is supposed to be a patch nominally identical to the ones describes in section 3.1, characterized by a nominal gain G_0, a nominal half beam angle θ_{HB} (degree) and a nominal Front to Back Ratio $F2B$ (dB). The elements are equally distributed around the node ($\theta_n = {}^{2\pi n}/_{N}$), and thus the same goes for the radiated beams.

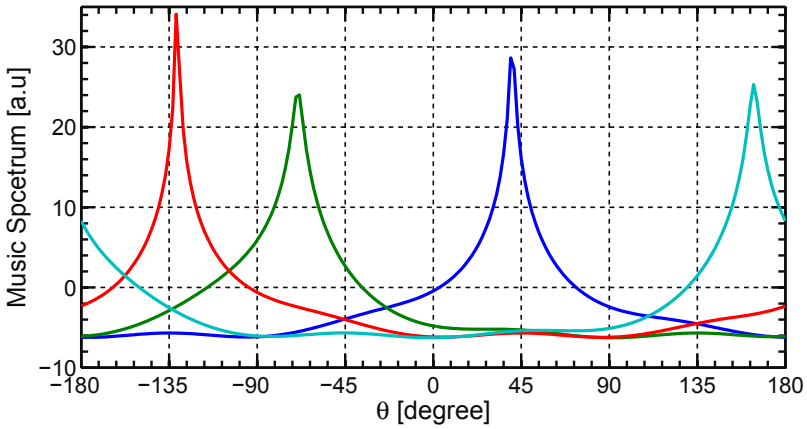

Figure 13. The four Music spectrum for the four anchors.

The target node, equipped with a 2D-omnidirectional antenna, can assume any arbitrary position in the area, identified by the 2D coordinates $(\bar{x}, \bar{y})$. The goal of the localization experiment is the given a position estimatation, indicated with $(\hat{x}, \hat{y})$, under various conditions of the anchors and the channel. The performance of the localization are evaluated on the basis of a localization error:

$$\epsilon = (\bar{x}, \bar{y}) - (\hat{x}, \hat{y}) \tag{21}$$

The first step of the localization procedure is the estimation of the four DoA's, labeled $\hat{\theta}_{i=1,4}$, individuated by the target respect to the four anchors. To fix the idea, the target coordinates are $P = (3, 4)$, a central area of the room. Each Anchor, composed by $N = 4$ antenna elements, performs the communication task on the basis of a scheduled activity. The RSSI collection and the following elaboration leads to a MUSIC spectrum, defined in the 1D angular range of the target. The four music spectra are illustrated in Figure13, where is evident the typical sharp behavior of MUSIC, consequence of its definition (see Eq. 19).

The formal estimation is identified with the maximum of the spectrum, which define a line of bearing. Instead of simply consider the intersection of four line of bearing, another approach

is proposed. A modified spectrum is derived after the music estimation. The analytical expression of this auxiliary spectrum is:

$$MAP_i(x,y) = \exp\left(-\left(\frac{\theta_i(x,y)-\hat{\theta}}{\sigma_\theta}\right)^2\right) \tag{22}$$

Where $\theta_i(x,y)$ is a function, defined respect to the i-th anchor, which map each point of the area to the azimuth angle θ seen by the anchor. This map is a function of the area and the anchor position, which are defined before the experiment, thus the map is build in a off-line preprocessing phase. The term σ_θ is taken proportional to the standard deviation of the RSSI message, in order to take account of the intrinsic uncertainty of the link model. This spectrum redefinition leads to the four *music maps*, plotted in Figure14. Each map has a radial behavior, with a linear region of high probability around the line of bearing, and a decreasing behavior departing from this straight line. The product of the four spectra generate a global music spectrum, which synthesize the information of the four anchors. The peak of the spectrum identifies the estimated position of the target, as depicted in Figure15. The advantage of this approach is that a single unreliable DoA estimation is filtered out by the product, while the intersection of two reliable estimation is exalted.

5.2. Sensor network

In typical wireless sensor network application, the localization involves computing the position of the set of numerous nodes in a 2D space. The nodes are supposed to be non interagent, i.e. they not collaborate for the localization service, but they neither interfere. According to the previous analysis we will use the same approach based on the music map. The procedure was evaluated by generating a 13×13 nodes network, regularly spaced in a grid of $8m \times 8\,m$ centered in the same $10 \times 10\,m$ area.

A first simulation is depicted in Figure16. The pathloss exponent is $n_p = 2$ and the σ_{RSSI} is 3 dB. The SBA anchors are made of $N = 4$ antenna elements are characterized by a gain $G_n = 3\,dB$ and a $\theta_{HB} = 50$, while the target is equipped with an regular 2D-omnidirectional antenna ($G_T = 0\,dB$). For each node of the network, a local error is computed as the euclidean norm of the distance between actual and estimated position. In Figure17 an histogram of the global computed errors is depicted. To summarize, with the described condition, a mean absolute error of $0.75\,m$ ($mean_x = 0.51\,m$, $mean_y = 0.50\,m$) and a max absolute error of $1.80\,m$ ($max_x = 1.5\,m$, $max_y = 1.3\,m$) is evaluated. As expected, the minimal error condition is around the center of the area, where the four anchors show the best collaboration effect. The nodes located too close to one of four anchors suffers for a biased estimation, as testified by the error arrows. This was expected, since the combination of the four map is unbalanced. Nevertheless, the error seems systematic, thus eventually resolvable.

To pursue a deeper investigation, a set of experiment was taken with a statistical variation of σ_{RSSI}. The localization performance are expected to aggravate as the standard deviation – and so the noise level – increases. In Figure18(a), the mean and max errors are computed as σ_{RSSI} increases from 0 to 15 dB. From a simple inspection is clear that both of them grow with a regular monotonic behavior, maintaining almost the same ratio of the max error ranging from 2 to 3 times the level of the mean error.

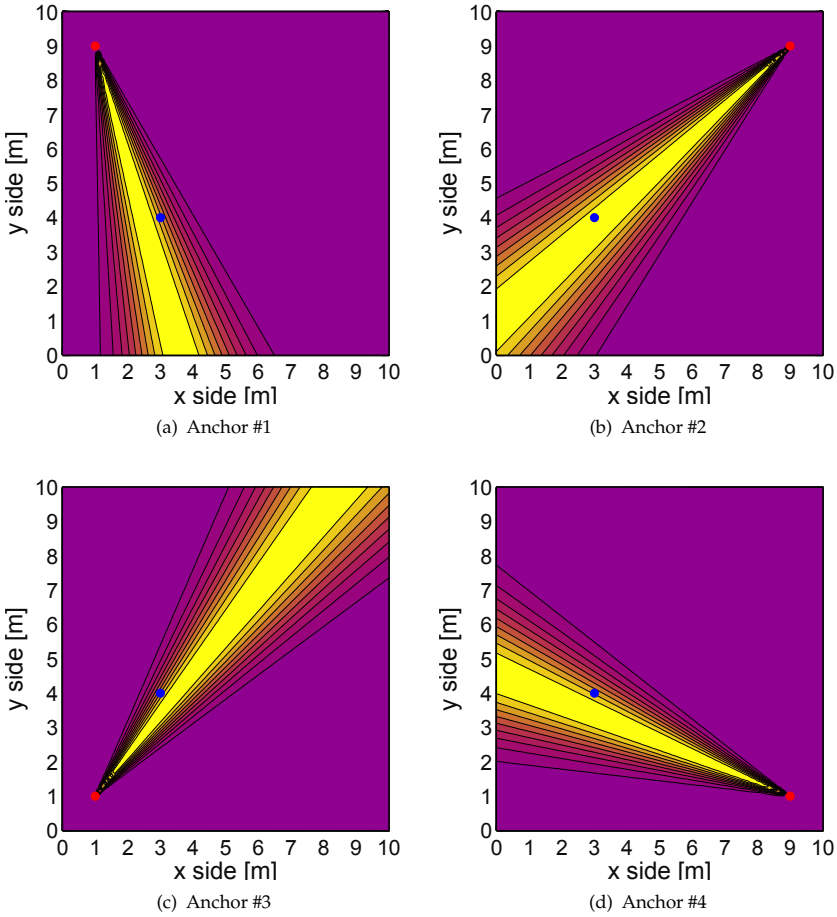

(a) Anchor #1 (b) Anchor #2

(c) Anchor #3 (d) Anchor #4

Figure 14. Four 2D Music maps estimate the target DoA referred to the the four anchor nodes.

Another set of simulation was taken to confirm the behavior of Figure18(a). The simulation is similar, but with a different θ_{HB} value. A narrower beam is expected to improve the localization results, as the angular filtering effect helps the localization mechanism. Figure18(b) and Figure18(c) presents the case of $\theta_{HP} = 50, 70$. The plots confirm the spatial filtering behavior, where a narrower and wider beam lead respectively to a better and worst localization performance, in terms of both mean and max error. Analyzing this data, one can think that a very narrow beam could lead to an even better performance.

Unfortunately, an excessive directivity, hence an extreme beam narrowness, is not always appropriate. As a demonstration, Figure19(a) shows the mean and max localization error for a set of parametric simulation where the free parameter is θ_{HB}, while the σ_{RSSI} is set at 6 dB – adequate to describe a noisy indoor case – and the other geometric and physic

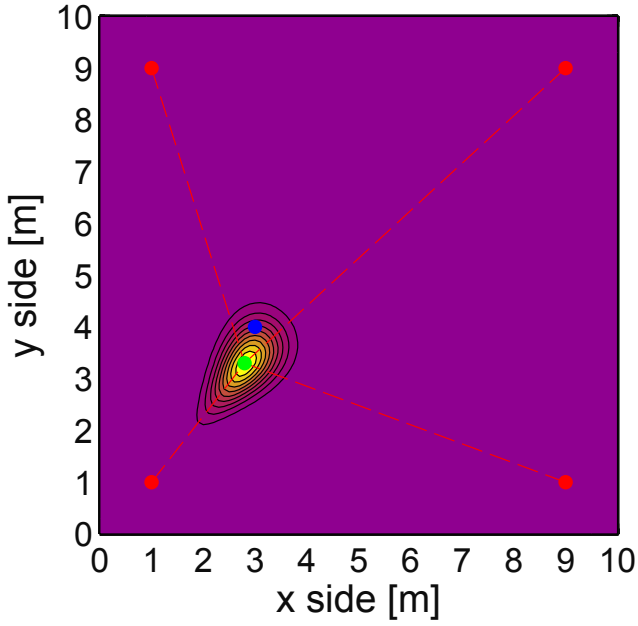

Figure 15. Localization based on the global music map with the four lines of bearing identifying the estimated position.

parameters are the same of the previous simulation. The localization error increases with θ_{HB}, confirming increasing error as the antenna beams enlarge, as expected for this class of DoA estimator. Paradoxically, when the beam is excessively narrow, the error cross a *critical point* where it experiments a absolute minimum, and then grows abruptly reaching an even higher peak. The physical reason lies in the fact that with extremely directive antenna, the angular range between two adjacent narrow beam peaks is low in absolute value, leaving an *uncover* area, where the signal became too weak, leading to an RSSI vector with a very low magnitude – ||RSSI|| – and thus heavily corrupted by the random noise. For the positioning algorithms this is an unbearable condition, where the estimation is affected by a very low accuracy. Figure11(b) and 11(c) depict an optimal situation, where the cumulative pattern covers the entire 2π domain with a maximum small ripple of 3 dB. The case of Figure11(a), while still satisfying, begins to show the problem of excessive directivity. As a further proof of this behavior, the same simulated experiment described by Figure19(a) is repeated in a bigger area of $20 \times 20\,m$. The results of the simulation are depicted in Figure19(b), where the mean and max error are almost doubled.

To avoid this issue, the directivity by itself is not a solution. A better condition is achieved if each antenna element is directive, but at the same time the cumulative pattern of the entire antenna set should show an isotropic coverture, as expressed in section 3. This ensure an RSSI vector whose norm ||RSSI|| is always meaningful, stronger than the noise. To demonstrate this

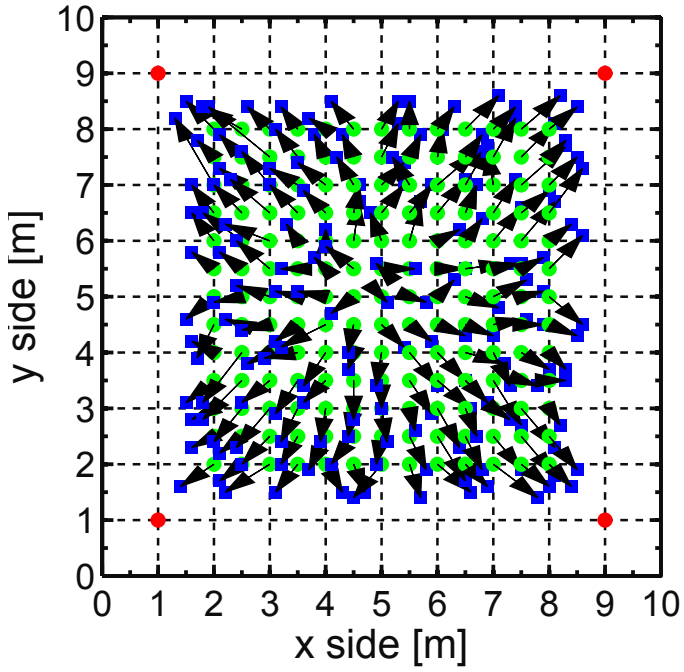

Figure 16. Localization of wireless senor network in a indoor area. The dots represent the actual position, while the square are the estimated positions.

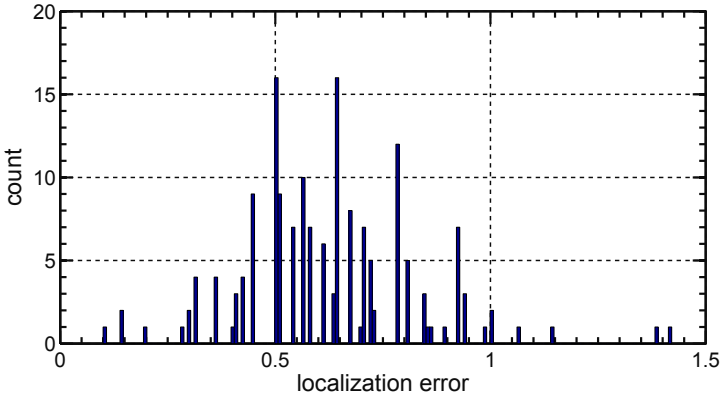

Figure 17. Localization error histogram for the simulation results of Figure16.

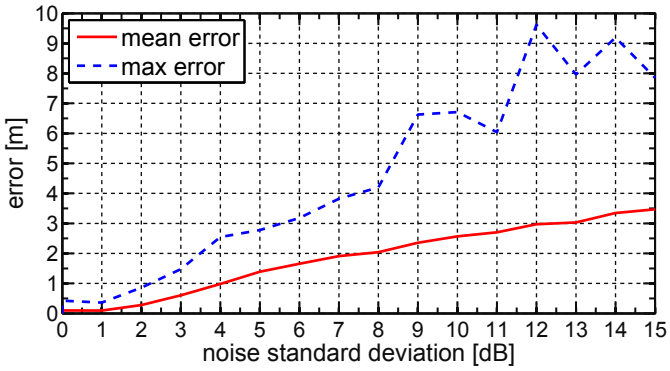

(a) $\theta_{HB} = 30$

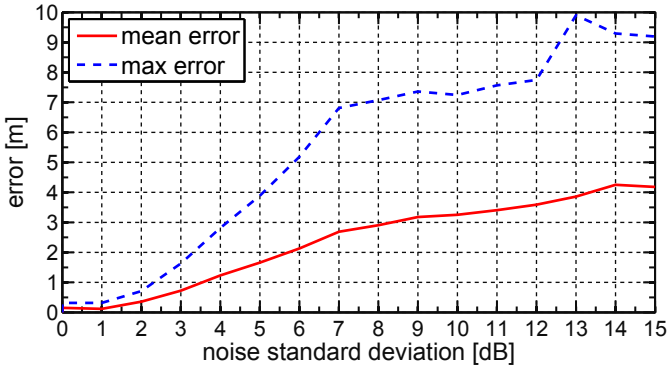

(b) $\theta_{HB} = 50$

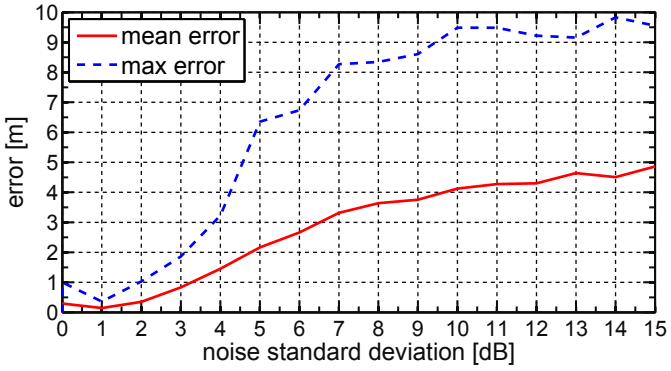

(c) $\theta_{HB} = 70$

Figure 18. Various simulated experiments showing the influence of σ_{RSSI} and θ_{HB} on the mean and max error.

condition, another set of simulation is presented in Figure20. In this case all the conditions are taken constant, with a θ_{HB} equal to 20 degrees and $\sigma_{\text{RSSI}} = 6\,dB$. The free parameter is the antenna number N. As expected, the mean decreases as N grows, and so does the max error, confirming the positive contribute of an increased set of antenna. When N passes a threshold, the contribute of another antenna is ininfluent, leading to a saturated error level. Not only: too much antenna element make the SBA cumbersome, making the SBA unfeasible for various aspects. As a final proof, the same simulation described in Figure20 was repeated with N = 6.

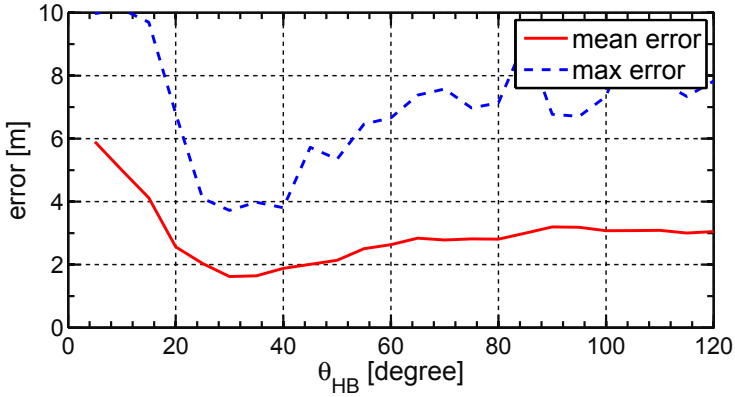

(a) $10\,m \times 10\,m$

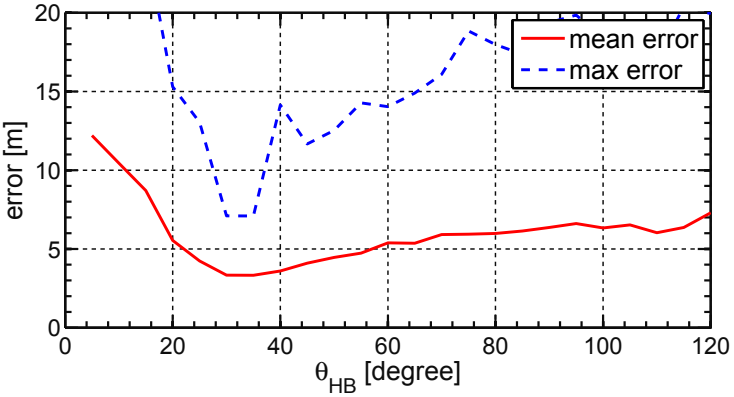

(b) $20\,m \times 20\,m$

Figure 19. Mean and max localization error vs θ_{HB}. N = 4, $\sigma_{\text{RSSI}} = 6\,dB$.

A similar error plot is obtained, but with a lower critical point and a more extreme divergence. With a choice of $\theta_{HB} = 20$, the optimal performance of $mean_{err} = 35\,cm$ are achieved. With the aid of these kind of plot is possible to choose the better parametric condition to ensure a satisfing error level for the application in exam.

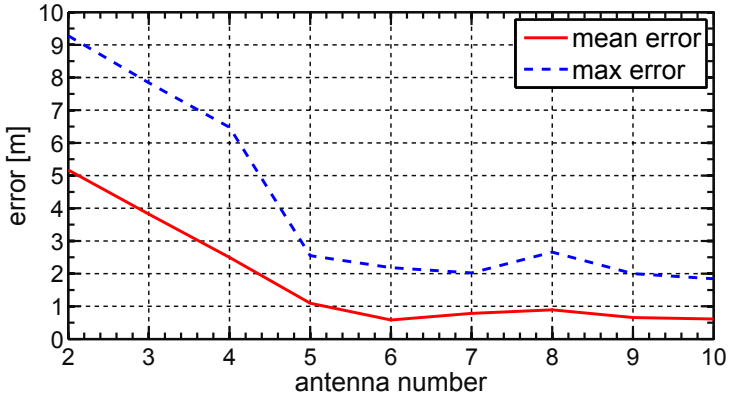

Figure 20. Mean and max localization error vs N. $\theta_{HB} = 20$ degrees, $\sigma_{\text{RSSI}} = 6\,dB$.

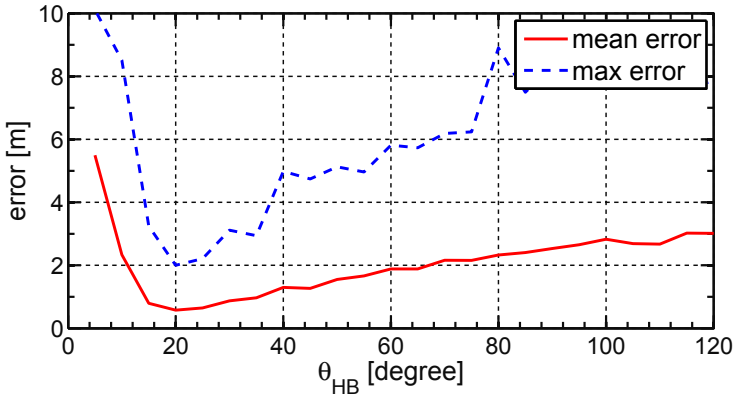

Figure 21. Mean and max localization error vs θ_{HB}. N = 6, $\sigma_{\text{RSSI}} = 6\,dB$.

6. Conclusions

In this paper, the concepts for an indoor localization system suitable for a Wireless Sensor Network in a GPS-denied scenario was presented. The localization of sensor nodes in a necessary tasks to give position-awareness to the nodes, a physical information leading to a vast range of impacting applications. The problem was addressed in terms of systemic approach, suitable hardware, consequent algorithm and estimated performance.

The proposed localization system is based on the Direction of Arrival approach, implemented manipulating Radio Signals. The position of a generic sensor node in the network is estimated on the basis of its RF communication with a master node, without the need of other spatial sensors. Equipped with a complex switched beam antenna, The master node serves as anchor. The localization algorithm relies on the collaboration of a set of anchor nodes, responsible of independent DoA estimations. The proposed algorithm operates on the RSSI-meter, the coarse power meter embedded in almost all the modern commercial wireless devices. In particular,

the CC2430 System-on-a-Chip was individuated as the best hardware for the master and the sensor nodes.

Range measurement are extremely inaccurate in indoor area, making traditional range-based algorithm like trilateration fail in hostile area like complex indoor environments. The RSSI data, while affected by numerous noise sources, are suitable for the Direction of Arrival algorithm, which is a *range-free* algorithm, an approach which does not rely on range estimation. The results showed in this paper have demonstrated that a WSN system made of COTS-based nodes is suitable for in-door positioning service. A wide dynamic of cases, with a punctual correlation to the physic and statistical parameters, gives a exemplary design principle for the structure of the nodes, with particular emphasis on sub-antenna system.

Author details

Stefano Maddio, Alessandro Cidronali, Gianfranco Manes
Department of Electronics and Telecommunication - University of Florence, Via S. Marta 3, 50139 Florence, Italy

7. References

[1] Akyildiz, I., Su, W., Sankarasubramaniam, Y. & Cayirci, E. [2002]. A survey on sensor networks, *Communications magazine, IEEE* 40(8): 102–114.
[2] Arora, A., Dutta, P., Bapat, S., Kulathumani, V., Zhang, H., Naik, V., Mittal, V., Cao, H., Demirbas, M., Gouda, M. et al. [2004]. A line in the sand: a wireless sensor network for target detection, classification, and tracking, *Computer Networks* 46(5): 605–634.
[3] Ash, J. & Potter, L. [2004]. Sensor network localization via received signal strength measurements with directional antennas, *Proceedings of the 2004 Allerton Conference on Communication, Control, and Computing*, pp. 1861–1870.
[4] Carver, K. & Mink, J. [1981]. Microstrip antenna technology, *Antennas and Propagation, IEEE Transactions on [legacy, pre-1988]* 29(1): 2–24.
[5] Cidronali, A., Maddio, S., Giorgetti, G., Magrini, I., Gupta, S. & Manes, G. [2009]. A 2.45 ghz smart antenna for location-aware single-anchor indoor applications, *Microwave Symposium Digest, 2009. MTT'09. IEEE MTT-S International*, IEEE, pp. 1553–1556.
[6] Cidronali, A., Maddio, S., Giorgetti, G. & Manes, G. [2010]. Analysis and performance of a smart antenna for 2.45-ghz single-anchor indoor positioning, *Microwave Theory and Techniques, IEEE Transactions on* 58(1): 21–31.
[7] Djuknic, G. & Richton, R. [2001]. Geolocation and assisted gps, *Computer* 34(2): 123–125.
[8] Garg, Bahl, I. [2001]. *Microstrip Antenna Design Handbook*, Artech House.
[9] Giorgetti, G. [2007]. *Resource-Constrained Localization in Sensor Networks*, PhD thesis, Universita' Degli Studi di Firenze, Italy.
[10] He, T., Krishnamurthy, S., Stankovic, J., Abdelzaher, T., Luo, L., Stoleru, R., Yan, T., Gu, L., Hui, J. & Krogh, B. [2004]. Energy-efficient surveillance system using wireless sensor networks, *Proceedings of the 2nd international conference on Mobile systems, applications, and services*, ACM, pp. 270–283.
[11] Hittite [2012]. *http://www.hittite.com/*.
[12] Hofmann-Wellenhof, B., Lichtenegger, H. & Collins, J. [1993]. Global positioning system. theory and practice., *Global Positioning System. Theory and practice., by Hofmann-Wellenhof,*

B.; Lichtenegger, H.; Collins, J.. Springer, Wien (Austria), 1993, 347 p., ISBN 3-211-82477-4, Price DM 79.00. ISBN 0-387-82477-4 (USA). 1.

[13] Krim, H. & Viberg, M. [1996]. Two decades of array signal processing research: the parametric approach, *Signal Processing Magazine, IEEE* 13(4): 67–94.

[14] Maddio, S., Cidronali, A., Giorgetti, G. & Manes, G. [2010]. Calibration of a 2.45 ghz indoor direction of arrival system based on unknown antenna gain, *Radar Conference (EuRAD), 2010 European*, IEEE, pp. 77–80.

[15] Maddio, S., Cidronali, A. & Manes, G. [2010]. An azimuth of arrival detector based on a compact complementary antenna system, *Wireless Technology Conference (EuWIT), 2010 European*, IEEE, pp. 249–252.

[16] Maddio, S., Cidronali, A. & Manes, G. [2011]. A new design method for single-feed circular polarization microstrip antenna with an arbitrary impedance matching condition, *IEEE Transactions on Antennas and Propagation* 59(2): 379–389.

[17] Malhotra, N., Krasniewski, M., Yang, C., Bagchi, S. & Chappell, W. [2005]. Location estimation in ad hoc networks with directional antennas, *Distributed Computing Systems, 2005. ICDCS 2005. Proceedings. 25th IEEE International Conference on*, IEEE, pp. 633–642.

[18] Mukhopadhyay, S. [2012]. *Smart Sensing Technology for Agriculture and Environmental Monitoring*, Vol. 146, Springer Verlag.

[19] Patwari, N., Ash, J., Kyperountas, S., Hero III, A., Moses, R. & Correal, N. [2005]. Locating the nodes: cooperative localization in wireless sensor networks, *Signal Processing Magazine, IEEE* 22(4): 54–69.

[20] Schantz, H. [2011]. On the origins of rf-based location, *Wireless Sensors and Sensor Networks (WiSNet), 2011 IEEE Topical Conference on*, IEEE, pp. 21–24.

[21] Schmidt, R. [1986]. Multiple emitter location and signal parameter estimation, *Antennas and Propagation, IEEE Transactions on* 34(3): 276–280.

[22] Werner-Allen, G., Lorincz, K., Ruiz, M., Marcillo, O., Johnson, J., Lees, J. & Welsh, M. [2006]. Deploying a wireless sensor network on an active volcano, *Internet Computing, IEEE* 10(2): 18–25.

[23] Yick, J., Mukherjee, B. & Ghosal, D. [2008]. Wireless sensor network survey, *Computer networks* 52(12): 2292–2330.

[24] Zekavat, R. & Buehrer, R. [2011]. *Handbook of Position Location: Theory, Practice and Advances*, Vol. 27, Wiley-IEEE Press.